An Unobstructed View of Liquid Flow in Structured Packing

Marc Wehrli[a,*], Thilo Kögl[b], Thomas Linder[b], Wolfgang Arlt[b]

[a]Sulzer Chemtech Ltd, CH-8404 Winterthur, Switzerland
[b]Institute of Separation Science and Technology, Friedrich-Alexander-University Erlangen-Nürnberg, D-91058 Erlangen, Germany
marc.wehrli@sulzer.com

The liquid distribution on the surface of structured packing, the holdup and the relative interfacial area are investigated using X-ray computed tomography (CT). Packed columns of two different inner diameters 100 mm and 200 mm are used and the fluid dynamics for Mellapak[TM] of two different specific geometric areas are explored. Three-dimensional information is obtained by means of a helical scan. Despite deviations in the holdup profiles in detail, there is a good agreement between the average holdup and average relative interfacial area of Mellapak 500.Y measured in the two column diameters. Therefore, the 100 mm data of Mellapak 500.Y and the 200 mm data of Mellapak 250.Y are generally valid, and information is transferrable to larger column diameters. Relative interfacial area does not scale according to the liquid line load. Geometric features of the packings affect the flow morphology significantly, and in such a way that geometric similarity cannot be claimed for the two packings.

1. Introduction

Capturing the fluid dynamics inside structured packing is difficult due to opaque walls that obstruct the view and render the inside inaccessible for instrumentation. Nevertheless, methods were developed as early as 1972 (Zogg) to visualize the single-phase bulk flow between arrays of crossing channels. But details related to the liquid film flow on the packing surface remained obscure for a long time. Kohrt et al. (2011) investigated the local effect of the surface texture on liquid film flow and its influence on liquid-side mass transfer.

Traditionally, the interfacial area is determined indirectly by a series of absorption experiments (Tsai et al., 2011). This method is suitable to determine a viable set of mass transfer parameters and to compare different packing types. But local information about internal liquid spreading remains inaccessible. Radiography (Süess and Spiegel, 1992) can provide holdup information, but again, not on the desired local scale.

For a long time, Computational Fluid Dynamics (CFD) was expected to offer the missing information. But progress in the field of two-phase flow is slow. Encouraging results have recently been reported by Olenberg and Kenig (2017). Then again, tomography has been successfully applied since the first endeavours in the late nineties. For a review, see Schubert et al. (2011). Janzen et al. (2013) used tomography to investigate and classify the flow morphology in Sulzer MellapakPlus[TM] 752.Y. Schug and Arlt (2016) investigated Sulzer Mellapak[TM] 500.Y and the effect of surface texture in a column of 100 mm inner diameter using high resolution X-ray computer tomography (CT). They revealed generally a lower holdup than radiography by Süess and Spiegel (1992). Liquid flows predominantly in rivulets, and a two-dimensional simplified Nusselt-type falling film model on a fully wetted wall is not applicable to predict the average film thickness in the packing. Green et al. (2007) investigated the water and air counter-current flow in a column of 146 mm diameter using CT and were able to capture characteristic information over a wide range of operating data including flooding phenomena. For Mellapak 250.Y their holdup and interfacial area values agreed well with data obtained using conventional methods. The present investigation aims at substantiating previous findings of Schug and Arlt (2016), now at a larger column inner diameter of ID = 200 mm. Two packings of different specific geometric area shall be compared for both liquids water and isopropanol. The following questions are specifically addressed: Is the available diameter sufficient to provide a representative picture of liquid flow in the packing? Is line load a useful criterion to predict the achievable wetting of the packing surface, in other words: can geometric similarity be established for the hydraulics of Mellapak of differing specific area?

2. Methods

2.1 CT Scanner

The industrial CT scanners used by Green et al. (2007) or Janzen et al. (2013) required the packed column to rotate. The present scanner known from Schug and Arlt (2016) rotates around the object and offers superior resolution. It is a third-generation fan beam tomographic setup, consisting of one X-ray source and a detector array mounted on a gantry system. The setup allows for a measurement volume up to 300 mm diameter and 1000 mm height. The X-ray tube is operated at an acceleration voltage of 140 kV. The detector of 480 mm length and 5566 pixels allows for a theoretical spatial resolution of 81 μm × 81 μm × 57 μm. The projections are acquired at a uniform exposure time of 2 ms.

Tomographic measurements of the structured packing are performed in two complementary modes: 2D scans offer a high temporal resolution of 0.7 frames per second, whereas helical 3D scans allow for flow morphology analysis at a lower temporal resolution.

In the case of 2D scans, the source-detector assembly rotates around the object at constant height as illustrated top of Figure 1a. One revolution is achieved, and 750 projections are recorded in 1.5 second resulting in one cross-sectional image. The computer programs ImageJ (Schneider et al. 2012) and Matlab (Trademark of The MathWorks, Inc.) are used to further process the raw images of 1533 × 1533 or 3301 × 3301 pixels (for ID = 100 or 200 mm) resulting from a filtered back projection reconstruction algorithm. The gray value scale distinguishes between ranges that can be assigned to background noise and the signals obtained from the packing, the liquid and the column wall. The position of the packing sheets can be identified easily, but the sheets are blurred due to beam hardening. However, the packing geometry can be easily reconstructed as the orientation and the thickness of the metal sheets are both known. Relevant parameters like holdup and interfacial area can be directly retrieved out of segmented images as described by Schug and Arlt (2016).

In the case of 3D tomographic scans, the rotating source-detector assembly continuously moves along the vertical axis. The detector describes a helical path around the column as illustrated bottom of Figure 1a. The so acquired raw projections get directly reconstructed into a three-dimensional voxel grid. To reconstruct the complete packing volume several hundred rotations of the scanner are required. The full volume scan of a packing element of 200 mm height takes about 1.5 h. In case of an unsteady liquid flow the resulting 3D image combines therefore an inconsistent sequence of snapshots. Despite this limitation, it may still be useful for a qualitative assessment of the flow. The reconstruction is implemented in Matlab based on the open source ASTRA Toolbox (van Aarle et al., 2015) designed for acceleration by means of the GPU.
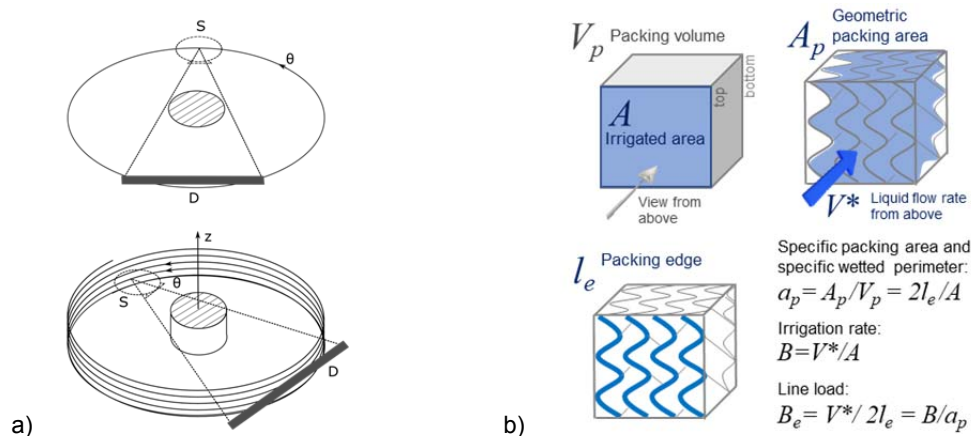

Figure 1: a) Tomographic scan geometry for 2D (top) and helical 3D scan (bottom); abbreviations: S: X-ray source, D: detector, Θ: rotation angle, z: vertical axis. b) Definition of parameters in the context of packing irrigation. The packing edge l_e is obtained by summing up the edges of all packing sheets at the top of the packing element. Parameters a_p and B_e require 2 × l_e because both sides of the metal sheets are irrigated.

2.2 Experimental Setup of the Column

Before installation, the packing elements were dried and cleaned by means of boiling acetone. Five elements of approximate 200 mm height were packed into the glass column. A pipe distributor with 7 drip points was installed on top of the packing bed of ID = 200 mm, and 4 drip points were present in the 100 mm column. The resulting distribution density over the column cross section A is more than 200 m^{-2} in the first case and more than double that value in the second case. The column is fed with water or isopropanol at selected loads

resulting in two irrigation rates B = 10 and 20 m³/m²h. From the bottom of the column the liquid returns to the storage tank and is pumped back to the top. The primary interest of this investigation is the free development of liquid flow inside the packing. It is known that liquid remains unaffected by gas flow over a large range of F-factor, provided it is below the Loading Point (Duss, 2006). Most measurements are therefore carried out at zero gas load F = 0. A few pre-tests with an F-factor of 0.8 Pa$^{0.5}$, using controlled injection of saturated pressurized air, confirmed this independency. Air is used with water and nitrogen with isopropanol.

Sulzer Mellapak structured packing is used with two different specific geometric areas: Mellapak 500.Y and Mellapak 250.Y with a_p = 500 m²/m³ and 250 m²/m³, respectively. They are made of dimpled and perforated aluminium sheets of 45° corrugation angle and triangular channels. Adjacent sheets touch each other at contact points that lie on crests and valleys respectively. Due to the different specific geometric areas a_p, channels of the first packing have a width approximately half the size of those of the second. This time, and complementary to Schug and Arlt (2016), a larger column diameter of ID = 200 mm is selected. Therefore, the elements of Mellapak 500.Y and Mellapak 250.Y comprise 28 and 16 adjacent corrugated sheets, respectively. Installing the second packing in a column of only 100 mm would result in only 7 sheets. The ratio of column diameter to channel width would diminish to less than the critical value of ten, and wall effects would for sure dominate the fluid dynamics. By comparing results of Mellapak 500.Y in two columns of (still rather small) 200 mm and 100 mm we will explore whether the smaller column is sufficiently large and 16 corrugated sheets lead to representative data. Could this fact be established successfully, one would conclude that ID = 200 mm is sufficiently large to obtain representative results with Mellapak 250.Y.

At identical irrigation rate B, the two packings experience a different line load B_e because of the different specific area. The line load is the liquid flow rate per unit width of wetted wall, which is commonly used in two-dimensional falling film theory (see Figure 1b for definitions). At B = 10 m³/m²h the line load is therefore B_e = 0.02 m³/mh for Mellapak 500.Y and B_e = 0.04 m³/mh for Mellapak 250.Y. Under ideal conditions, high line load results in a thicker film. Under less favourable circumstances, wetting of the wall, holdup and relative interfacial area improve as line load increases. At the same irrigation rate, Mellapak 250.Y has an advantage over the packing with higher specific surface area. But wetting should be identical at the same line load.

2D scans are carried out over the whole bed length at intervals of 13 to 15 mm. Profiles are obtained by averaging each 2D scan, while overall characteristic numbers are the result of averaging over all 62 height positions. For the detailed visual inspection of the local flow, a 2D scan is taken at half height of the 4th element numbered from the top. The same element is selected for the 3D helical scan. For visualization of the liquid distribution, one of the two interior packing sheets next to the packing axis is then selected.
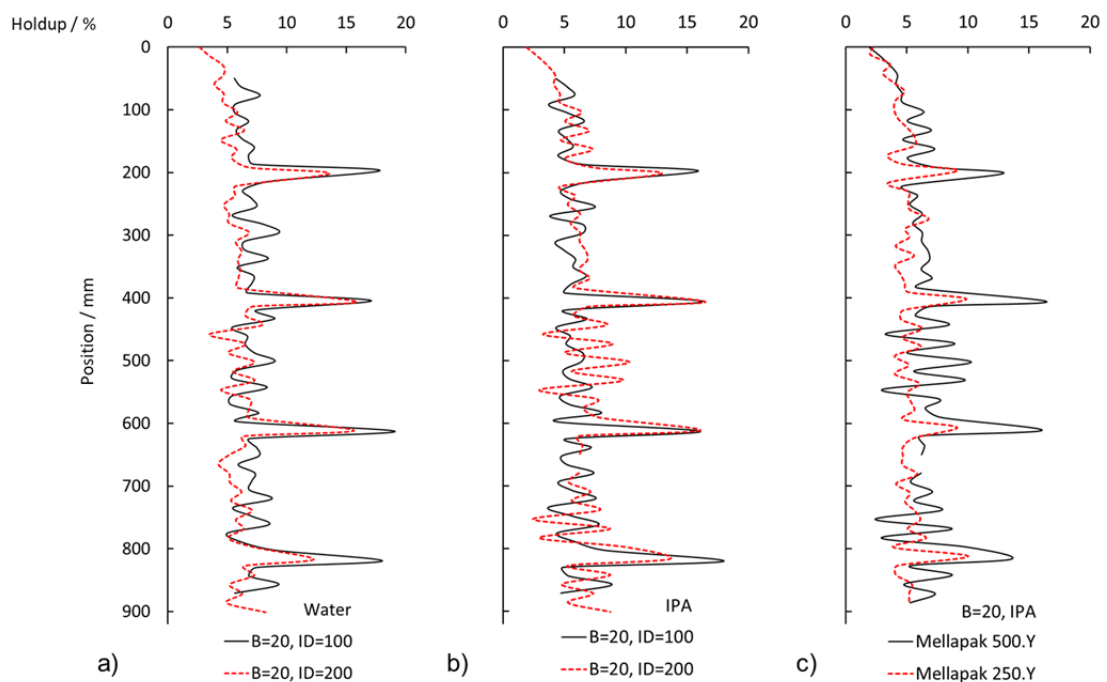

Figure 2: Holdup profiles along the packing bed at F = 0 and an irrigation rate of B = 20 m²/m³h. a) Mellapak 500.Y, water measured at ID = 200 mm and 100 mm. b) Mellapak 500.Y, isopropanol (IPA) at both IDs. c) Mellapak 500.Y and Mellapak 250.Y with isopropanol and ID = 200 mm.

3. Results and Discussion

3.1 Liquid holdup

The average holdup in the entire bed is shown in Figure 3a for both packings and both column diameters at two liquid loads. For ID = 200 mm there is almost no difference between the experimental holdup of water and isopropanol, even the holdup of isopropanol at the small ID of 100 mm is very similar. Only the holdup of water in the small column is high due to wall effects dominated by surface tension. The lines in Figure 3a represent the Süess and Spiegel (1992) correlation for water. In agreement with Schug and Arlt (2016), holdup for Mellapak 500.Y is lower than predicted. For Mellapak 250.Y, there is less deviation.

In Figures 2a and b holdup profiles are plotted against the packing height for Mellapak 500.Y, while Figure 2c compares both packings. Peaks of increased liquid holdup at the element interfaces are well visible, but they are confined to a very narrow space in the order of 20 mm. Due to the significantly lower resolution of the radiography method Süess and Spiegel (1992) were not able to detect such peaks at operating conditions below the Loading Point. The profile in the uppermost packing bed is determined by the distributor's irrigation pattern, rivulet flow and accordingly lower holdup. In the second element (between positions 200 and 400 mm), holdup is still increasing until it reaches its characteristic average value in the third element. The wavy shape of the profiles is due to the perforation of the packing sheets, characterized by rows of holes arranged uniformly at defined axial positions. As the X-ray positions are not aligned with the holes, only a part of the holes is hit. Such locations are distinguished by a low holdup, especially with isopropanol. Peaks inside the element are the result of liquid bulging in the neighbourhood of the holes. Water with its high surface tension is not entirely affected by the presence of holes and tends to flow over some. The profiles are therefore less wavy. The wavy structure of the ID = 100 mm and 200 mm profiles do not match because the experimental setup does not allow to bring perforation rows and scan elevations into full agreement. Nevertheless, the agreement of the profiles is better with isopropanol (Figure 2b) than with water (Figure 2a). Figure 2c juxtaposes holdup of both Mellapak 500.Y and Mellapak 250.Y measured in the 200 mm column. The different geometric areas suggest that the latter should have only half the holdup of the first packing. A fair comparison should be carried out at identical line load B_e. This is achieved by comparing the Mellapak 250.Y triangle of B = 10 m^3/m^{2}h with the blue filled circle of Mellapak 500.Y at B = 20 m^3/m^{2}h in Figure 3a. Apparently, Mellapak 250.Y with 4.4% has more than half the holdup of Mellapak 500.Y (6.6%).
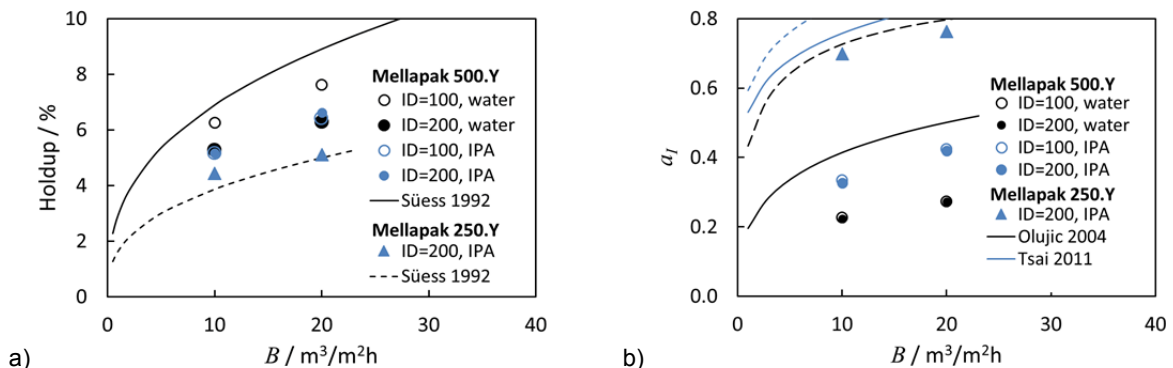

a)   b)

Figure 3: Hydraulic data at conditions below loading point for both packings. a) Measured holdup and correlation of Süess and Spiegel (1992) for water. b) Relative interfacial area and correlations of Olujic et al. (2004) with black lines, Tsai et al. (2011) with blue lines. Solid lines: water; dashed lines: isopropanol.

3.2 Interfacial area

Like holdup, the interfacial area shows a wavy progression along the height of the packing bed. The average relative interfacial area a_I is presented in Figure 3b. It is computed as $a_I = A_I/A_p$ the ratio of the interfacial area to the geometric area of a packing. The value of 1.0 would be desirable, but in the observed B range less than 0.5 is achieved for Mellapak 500.Y. The interfacial area achieved with isopropanol is significantly better than with water. For both liquids there is a good agreement between the values obtained in the small and the large column. Hence, the chosen range of column sizes is sufficient to substantiate diameter independence of the liquid distribution, and the ID = 200 mm provides almost scale independent information for Mellapak 250.Y.
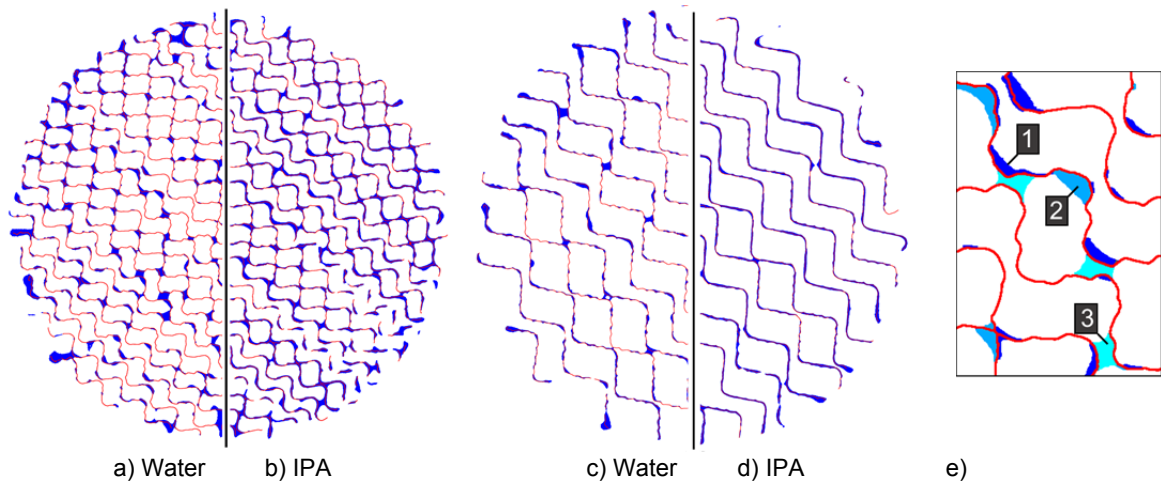
Figure 4: Representative CT images of one packing half at half height of the 4th packing element for B = 20 m³/m²h and F = 0. Mellapak 500.Y with water (a) and isopropanol (b), Mellapak 250.Y with water (c) and isopropanol (d). Examples for liquid films (1), rivulets (2) and bridges (3) in (e).
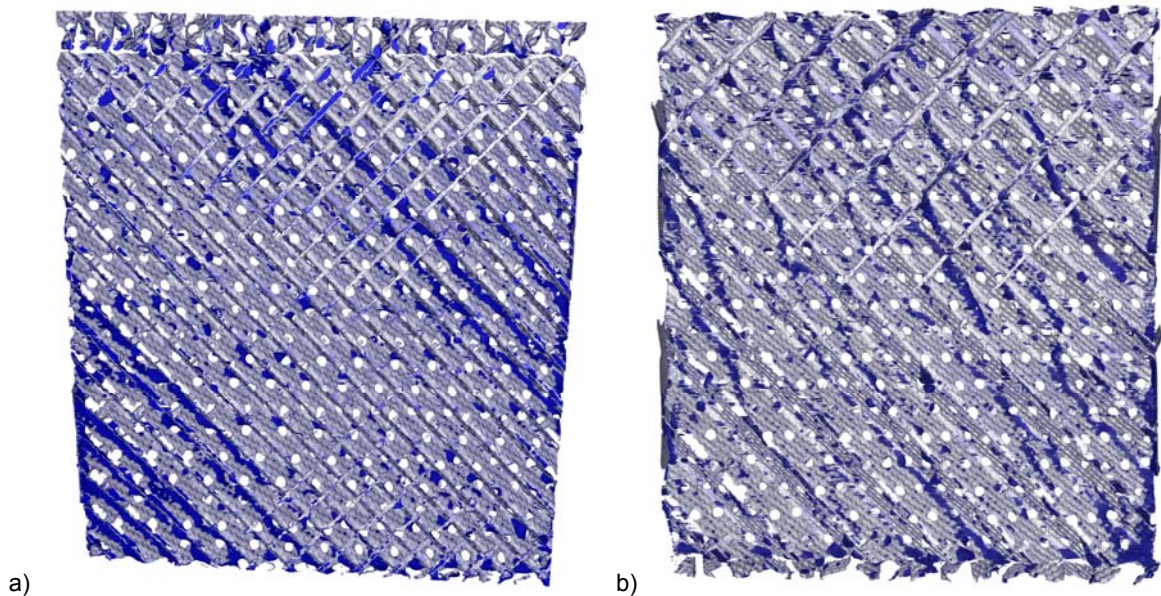

Figure 5: 3D tomographic data of the 4th packing element segmented and represented on one single packing sheet next to the packing axis, F = 0, B = 14 m²/m³h water. a) Mellapak 500.Y and b) Mellapak 250.Y

3.3 Flow morphology

At the same line load B_e, the initial conditions are equal for both packings such that identical wetting of the surface is achievable by theory. The relative interfacial area a_I of Mellapak 250.Y and Mellapak 500.Y should therefore be identical. But this is not the case. There must be other important effects, which are related to the geometry of the packing and the flow morphology. Inspired by Janzen et al. (2013), the liquid flow is characterized by patches with the form of liquid films, rivulets and bridges. Examples are highlighted in Figure 4e. Figures 4a to 4d show the different liquid distributions for water and isopropanol on representative half cross sections of the two packings. Water tends to accumulate and form bridges between metal sheets in the neighbourhood of contact points. Rivulets are formed in the hollow of the corrugation channels. In contrast to this observation, isopropanol nicely covers the surface by a film and achieves good wetting of the packing surface. While bridges and rivulets are still not entirely avoided in Figure 4b, Mellapak 250.Y in Figure 4d offers already almost a perfect liquid distribution. Hence, it is the different flow morphology of the packing with lower specific geometric area that explains the relatively high holdup and improved relative interfacial area.

Helical 3D tomographic scans as shown in Figure 5 are useful in assigning the individual patches of liquids (previously identified in Figure 4) to three-dimensional structures and understanding their connection to the larger scale liquid flow pattern. This analysis requires a detailed inspection of several pictures, but only two with water and B = 14 m^3/m^{2}h are presented here for illustration purpose. It becomes apparent that water covers the packing surface only to a small extent. In both pictures the typical accumulation of water close to the lower packing edge is visible, that causes the high holdup peaks. There is also accumulation of liquid on the left and right edges due to wall effects. The small-scale channels of Mellapak 500.Y seem to promote rivulet flow that aligns with the corrugation angle, whereas the larger channels of Mellapak 250.Y allow wider streams of water to follow a path with an inclination closer to the vertical and less affected by the presence of the corrugation. CFD simulations of Olenberg and Kenig (2017) for a packing with comparable geometric features show a similar sparse distribution of liquid, but the liquid tends to follow the channels more strictly. Differences may be explained by the absence of fine surface texture in their model.

4. Conclusions

The liquid flow of water and isopropanol in Sulzer structured packing Mellapak^{TM} 500.Y and Mellapak 250.Y was analysed using CT and two column diameters. For the first packing, average holdup and relative interfacial area at ID = 100 and 200 mm agree very well. Independency of the diameter can therefore be claimed for the tomographic data of Mellapak 500.Y obtained at ID = 100 mm and similarly for Mellapak 250.Y data at ID = 200 mm. Present observations are therefore meaningful and provide valuable insights transferrable to larger columns. At identical line load, holdup does not scale with the specific geometric area of two different packings. The relative interfacial area depends not on B_e, line load alone. Mellapak 250.Y shows better wetting characteristics than Mellapak 500.Y. The difference seems to relate to the channel width and the number of contact points. There exists no simple similarity relation for the liquid flow in both packings.

References

Duss M., 2006, A new method to predict the susceptibility to form maldistribution in packed columns based on pressure drop correlations, IChemE Symposium Series No. 152, Distillation and Absorption, London.

Green W.G, Farone J., Briley J.K., Eldridge R.B., Ketcham R.A., Nightingale B., 2007, Novel application of X-ray computed tomography: Determination of gas/liquid contact area and liquid holdup in structured packing, Ind. Eng. Chem. Res., 46 (17), 5734-5753.

Janzen A., Steube J., Aferka S., Kenig E.Y., Crine M., Marchot P., Toye D., 2013, Investigation of liquid flow morphology inside a structured packing using X-ray tomography, Chem. Eng. Sci., 102, 451-460.

Kohrt M., Ausner I., Wozny G., Repke J.U., 2011, Texture influence on liquid-side mass transfer, Chem. Eng. Res. Des., 89 (8), 1405-1413, DOI: 10.1016/j.cherd.2011.01.010.

Olenberg A., Kennig E.Y., 2017, Numerical Simulation of Two-phase Flow in Representative Elements of Structured Packings, Proceedings of the 27th European Symposium on Computer Aided Process Engineering – ESCAPE 27, October 1st – 5th, Barcelona, Spain, 2089-2094.

Olujić Ž, Beherens M., Colli L., Paglianti A., 2004, Predicting the efficiency of corrugated sheet structured packings with large specific surface area, Chem. Biochem. Eng. Q., 18, 89-96.

Schneider C.A., Rasband W.S., Eliceiri K.W., 2012, NIH Image to ImageJ: 25 years of image analysis, Nature methods, 9 (7), 671-675, PMID 22930834.

Schubert M., Bieberle A., Barthel F., Boden S., Hampel U., 2011, Advanced Tomographic Techniques for Flow Imaging in Columns with Flow Distribution Packings, Chem. Ing. Tech., 83 (7), 979-991.

Schug S., Arlt W., 2016, Imaging of Fluid Dynamics in a Structured Packing Using X-ray Computed Tompgraphy, Chemical Engineering & Technology, 39 (8), 1561-1569.

Suess P., Spiegel L., 1992, Hold-up of Mellapak structured packings, Chem. Eng. Process, 31, 119-124.

Tsai R.E., Seibert A.F., Eldridge R.B., Rochelle G.T., 2011, A dimensionless model for predicting the mass-transfer area of structured packing, AIChE J., 57, 1173-1184.

van Aarle W., Palenstijn W.J., De Beenhouwer J., Altantzis T., Bals S., Batenburg K.J., Sijbers J., 2015, A platform for advanced algorithm development in electron tomography, Ultramicroscopy, 157, 35-47, DOI: 10.1016/j.ultramic.2015.05.002.

Zogg M., 1972, Strömungs- und Stoffaustauschuntersuchungen an der Sulzer-Gewebepackung. PhD Thesis, Eidgenössische Technische Hochschule, Zürich, Switzerland.